A System of Two Piezoelectric Transducers and a Storage Circuit for Wireless Energy Transmission through a Thin Metal Wall

Hongping Hu, Yuantai Hu, Chuanyao Chen, and Ji Wang, *Senior Member, IEEE*

***Abstract*—A system to wirelessly convey electric energy through a thin metal wall is proposed in the paper, where 2 piezoelectric transducers are used to realize energy transformation between electric and mechanical, and a rechargeable battery is employed to store the transmitted energy. To integrate them as a whole, an interface of a modulating circuit is applied between the transducer system and the storage battery. In addition, a synchronized switch harvesting on inductor in parallel with the transducer system is introduced to artificially extend the closed interval of the modulating circuit. The process of transmitting energy is computed, and the performance of the transducer system is optimized in detail for a prescribed external electric source. The results obtained are useful for understanding and designing wireless energy supply systems.**

I. Introduction

There is a great challenge to supply energy for the electronic devices embedded inside sealed vessels, which are widely used in armor, spacecraft, nuclear reactors, dangerous chemicals containers, and so on. This is because the use of feed-through wires in such systems often brings some disadvantages, such as leakage, thermal or electrical insulation problems, and stress concentration [1].

In general, wireless energy supply techniques have 2 functions: one is to scavenge energy directly from the operating environment of electronic devices, for example, the scavenging of energy from ambient vibrations by piezoelectric energy harvesters [2]–[4]; the other is to convey power into sealed solid metallic structures without damaging the outer shells. Hu *et al.* [5], [6] and Yang *et al.* [7] proposed a wireless acoustic-electric transmission device consisting of 2 piezoelectric transducers. In the device, the outer transducer takes in electric energy from outer sources and transforms it into mechanical vibrations through the direct electromechanical coupling of piezoelectric ceramics. After receiving the vibrations, the inner transducer converts the mechanical energy into electric energy again via the converse piezoelectric effect. Sherrit *et al.* [8], [9] and Bao *et al.* [1], [10] investigated the energy loss of this transmission system by experiments and finite element computations. Saulnier *et al.* [11] and Primerano *et al.* [12] have used ultrasound piezoelectric transducers to study wireless communication through a solid steel wall, where the conventional radio frequency communications cannot be applied due to the shielding of the steel.

In general, a rechargeable battery is needed inside the sealed vessels to store the transmitted energy and to offer the electronic device a stable electrical source whenever necessary. Thus, a modulating circuit is applied as an interface between the piezoelectric transducer system and the battery. The modulating circuit is composed of a full-bridge rectifier and a dc-dc converter; the rectifier is to convert the alternate current of the inner transducer into a direct current, and the dc-dc converter is to match the rectified voltage with the battery voltage. A synchronized switch harvesting on inductor (SSHI) was often employed in the piezoelectric energy harvester. In the previous studies, lumped parameter models, described by ordinary differential equations (ODE), were often utilized to analyze the SSHI interface in piezoelectric energy harvesting [13], [14]. Theoretically, the motion of a piezoelectric continuum is governed by partial differential equations (PDE), which should be represented with a system of infinitely many ODE mathematically. And it is usually more complicated for PDE than ODE to construct the solutions, respectively, for closed and open phases with continuity at the transition moments of these 2 phases. Hence, it becomes far more complicated, particularly when a rectifier is applied. As for a piezoelectric device operating near resonance, a nonlinear analysis will be required [15]. In this research, we have concentrated our attention on how to realize the energy transmission wirelessly and the energy storage efficiently, so the resonant problem is left as future work. We present a mathematical formulation that governs thickness-stretch vibrations for the electric energy transmitting process under the excitation of a harmonic electric voltage source on the outer transducer; the numerical results are presented. Performance of the wireless energy supply system is optimized for a prescribed outer voltage source.

II. Governing Equations of Wireless Energy Supply System

To wirelessly convey energy into a battery sealed inside a closed vessel, an energy transmission system consist-

Manuscript received November 24, 2007; accepted May 21, 2008. This work was supported by the Chinese Postdoctoral Science Foundation (No. 20070410944).

H. Hu, Y. Hu, and C. Chen are with the Department of Mechanics, Huazhong University of Science and Technology, Wuhan 430074, China (e-mail: hudeng@263.net).

H. Hu is also with the School of Mechanical Science and Engineering, Huazhong University of Science and Technology, Wuhan 430074, China.

J. Wang is with the Piezoelectric Device Laboratory, School of Engineering, Ningbo University, Ningbo, 315211, China.

Digital Object Identifier 10.1109/TUFFC.930

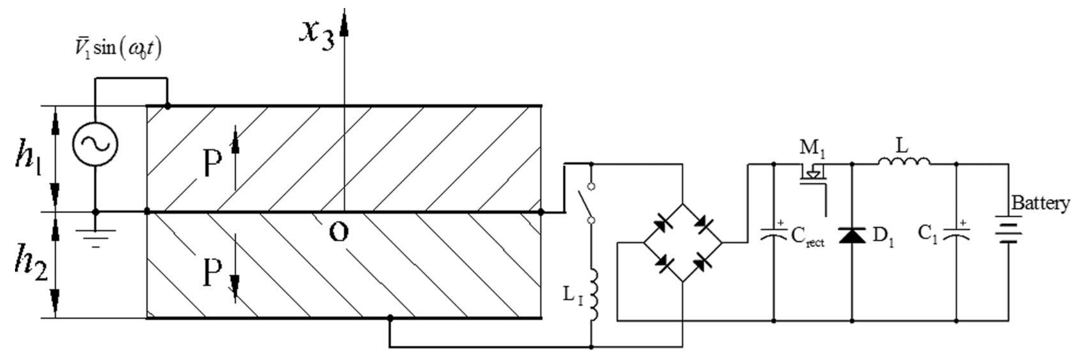

Fig. 1. A schematic illustration of the system consisting of 2 piezoelectric transducers and a storage circuit for wireless energy transmission through a thin metal wall.

ing of an energy transmitting element and a modulating circuit is proposed (see Fig. 1); the sealed wall has been simplified as an electrode considering that it is usually very thin. The energy transmitting element is composed of 2 piezoelectric layers: the top and bottom layers represent the transducers outside and inside the wall, respectively, and both are poled in different thickness directions. The 2 outer surfaces and the interface are electroded. The outer transducer is driven by a harmonic voltage source to generate longitudinal acoustic waves propagating along the x_3-direction. After receiving the mechanical vibrations from the sealed wall, the inner piezoelectric transducer transforms the mechanical vibrations into electric energy. To extend the closed circuit duration of the modulating circuit artificially, an inductor L_I followed by a switch (SSHI) is introduced in parallel with the inner transducer. The switch inside the SSHI is always open, except when a deformation extremum of the inner transducer occurs. The modulating circuit is composed of a full-bridge rectifier to convert alternate current into direct current with a capacitor C_{rect} as an energy transfer station and a dc-dc converter to match the rectified voltage V_{rect} of C_{rect} with the battery voltage V_b.

We note that the rectified capacitor C_{rect} should be much larger than the equivalent capacitance of the inner transducer, so that V_{rect} can be prescribed at a certain voltage that ensures the operation of the energy transmitting element at the optimal state. Obviously, the energy transmitting element is subjected to 3 types of electric boundary conditions: open and closed circuits and transition states from closed to open circuit. When the rectifier is open, the electric potential difference between the 2 output electrodes of the inner transducer is smaller than the rectified voltage V_{rect}, so that the inner transducer is with null output current. When the rectifier is closed, the output voltage of the energy transmitting element will be maintained at V_{rect} or $-V_{\text{rect}}$.

When the SSHI is in an on stage, i. e., a transition state from a closed to an open circuit, the inductor L_I and the equivalent capacitance C_p of the inner transducer constitute an oscillator to interchange charges between the 2 output electrodes of the inner transducer. If we choose the closed circuit interval of the L_I-C_p oscillator to be just equal to a half period of the oscillator $\pi\sqrt{L_I C_p}$, the switch will be kept closed until the output voltage of the inner transducer has been reversed.

We note that the operating process of such a wireless energy supply system includes 2 subprocesses: the energy transmitting process between the 2 piezoelectric transducers, and the energy storage process inside the storage circuit. Once V_{rect} is given, both the energy transmitting process and the energy storage process of the system shown in Fig. 1 can be determined separately.

We first consider the energy transmitting process. Motions of the piezoelectric transducers are governed by the following equations of linear piezoelectricity [16], [17]:

$$
\begin{aligned}
&T_{ji,j} + \rho f_i = \rho \ddot{u}_i, \quad D_{i,i} = 0,\\
&\qquad T_{ij} = c^E_{ijkl} S_{kl} - e_{kij} E_k, \quad D_i = e_{ikl} S_{kl} + \varepsilon^S_{ik} E_k,\\
&\qquad S_{ij} = \left(u_{i,j} + u_{j,i}\right)/2, \quad E_i = -\phi_{,i},
\end{aligned}
\tag{1}
$$

where u_i, E_i, and D_i are the components of the mechanical displacement, the electric field, and the electric displacement, respectively; T_{ij} and S_{ij} are the components of the stress tensor and the strain tensor, respectively; ϕ denotes the electric potential; c^E_{ijkl}, , e_{kij}, and ε^S_{ik} are the elastic, piezoelectric, and dielectric constants, respectively, where the superscripts E and S indicate that elastic and dielectric constants should be measured under the fixed electric field and the fixed strain condition, respectively; and ρ is the mass density. A superimposed dot represents time derivative. The Cartesian tensor notation, the summation convention for repeated tensor indices, and the convention that a comma followed by an index denotes partial differentiation with respect to the coordinate associated with the index are used.

Since the dimension in the thickness direction is much smaller than the in-plane dimensions, all variables can be regarded as independent of the in-plane coordinates, x_1 and x_2, by assuming the edge effect to be negligible. In the following, the compact notation is used and superscripts are removed for simplicity. From (1), the governing equation and the electric displacement equation can be obtained for thickness-stretch vibrations of the piezoelectric layers as follows:

$$\begin{aligned} \bar{c}_{33} u_{,3,33} &= \rho \ddot{u}_3, \\ D_{3,3} &= 0, \end{aligned} \tag{2}$$

where $\bar{c}_{33} = c_{33}\,[1 + e_{33}^2/(\varepsilon_{33} c_{33})]$ is the piezoelectric stiffened elastic constant. The linear piezoelectric constitutive equations for the outside transducer can be written as

$$\begin{aligned} T_{33} &= c_{33} u_{3,3} + e_{33} \phi_{,3}, \\ D_3 &= e_{33} u_{3,3} - \varepsilon_{33} \phi_{,3}. \end{aligned} \tag{3}$$

Since the poling direction is opposite to the x_3-direction in the inner transducer, its constitutive equations become

$$\begin{aligned} T_{33} &= c_{33} u_{3,3} - e_{33} \phi_{,3}, \\ D_3 &= -e_{33} u_{3,3} - \varepsilon_{33} \phi_{,3}. \end{aligned} \tag{4}$$

The boundary conditions of this structure are

$$\phi(h_1, t) = \bar{V}_1 \sin \omega_0 t, \quad T_{33}(h_1, t) = 0, \quad T_{33}(-h_2, t) = 0, \tag{5}$$

where ω_0 is the circular frequency of the harmonic voltage source with period $T_0 = 2\pi/\omega_0$. The interface between the outside and inner transducers is connected with the earth; the continuous conditions here are

$$\begin{aligned} &\phi(0^+) = \phi(0^-) = 0, \quad u_3(0^+) = u_3(0^-), \\ &T_{33}(0^+) = T_{33}(0^-). \end{aligned} \tag{6}$$

The electric charge Q_p per unit area on the bottom electrode surface of the inner transducer is given by

$$Q_p = D_3, \quad \text{on} \quad x_3 = -h_2. \tag{7}$$

The electric boundary condition acting on the inner transducer is determined by the on/off state of the rectifier as follows:

1) During an off state, $|V_p| < V_{\text{rect}}$ and

$$i_p = 0. \tag{8}$$

2) During an on state,

$$|V_p| = V_{\text{rect}}. \tag{9}$$

3) During a transition stage from closed to open circuit, we obtain the governing equation of charge interchange between the 2 output electrodes of the inner transducer by analyzing the $L_I - C_p$ oscillator as follows:

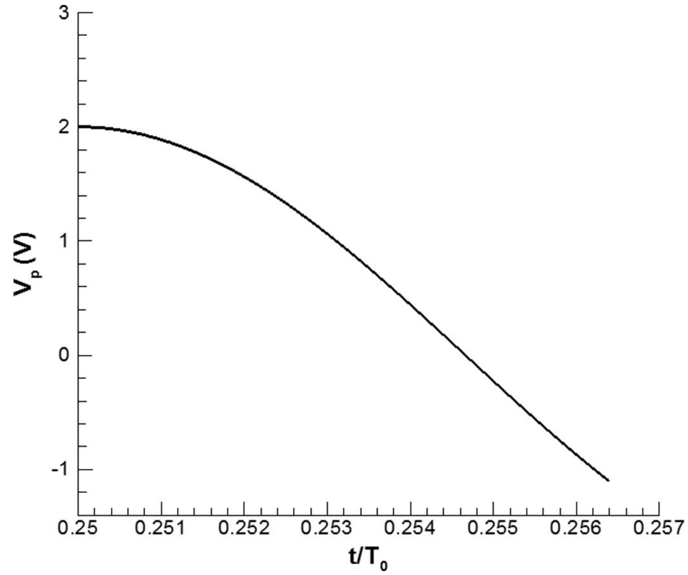

Fig. 2. Output voltage, V_p, of the inner transducer versus time over a transition stage.

$$L_I \frac{d^2 q}{dt^2} + \frac{q}{C_p} + V_{\text{oc}} \sin \omega_0 t = 0, \tag{10}$$

where V_{oc} is the voltage amplitude of the open circuit. Since the transition stage is far shorter than the other stages $(\pi\sqrt{L_I C_p} \ll T_0)$, a transition process is plotted alone in Fig. 2 to show inversion of the output voltage, V_p, of the inner transducer, where $V_{\text{rect}} = 2$ V, $L_I = 1$ pH. We note that the voltage inversion is not perfect because a part of the energy stored on the inner transducer capacitance is lost by the high frequency radiation due to the sharp edges of the voltage signal. Therefore, a quality factor Q can be defined for this degrading in the inversion oscillating network. We set the quality factor Q equal to 2.6, which corresponds to a preliminary experimental setup [13]. During a transition stage from a closed to an open circuit, output voltage of the inner transducer changes from V_{rect} to $-V_{\text{rect}} e^{-(\pi/2Q)}$, or from $-V_{\text{rect}}$ to $V_{\text{rect}} e^{-(\pi/2Q)}$, after charge interchanging between the 2 output electrodes of the inner transducer. Because $|\pm V_{\text{rect}} e^{-(\pi/2Q)}| < V_{\text{rect}}$, an open circuit stage of the rectifier follows the transition stage.

In addition, we need to take into account the continuous conditions of displacements and velocities of the structure at the transition point from the off to the on state, or from on to off of the rectifier. Obviously, $t = T_0/4$ and $3T_0/4$ are the instants of the rectifier from on to off. Designating t_1 and $t_1 + T_0/2$ as the moments of the rectifier from off to on, we therefore have

$$u_3^o(x_3, t_1) = u_3^c(x_3, t_1), \quad \dot{u}_3^o(x_3, t_1) = \dot{u}_3^c(x_3, t_1), \tag{11}$$

and

$$\dot{u}_3^o\left(x_3, T_0/4\right) = 0, \quad \dot{u}_3^c\left(x_3, 3T_0/4\right) = 0, \tag{12}$$

where superscripts "o" and "c" represent the quantities of the off and on states, respectively.

We define the output power of this structure as

$$P = \frac{1}{T_0}\int_0^{T_0} V_p i_p dt, \tag{13}$$

and define an average rectified current, for the requirement in designing proper circuit parameters, as follows:

$$\langle I_{\text{rect}}\rangle = \frac{1}{T_0}\int_0^{T_0} |i_p| dt. \tag{14}$$

Next, the charging behavior of a chargeable battery is analyzed. The charging current and voltage of a chargeable battery versus time are as follows [3], [4]:

$$\begin{aligned} V_b(s) &= V_\infty + \left(V_0 - V_\infty\right)e^{-\alpha s}, \\ i_b(s) &= \begin{cases} I_0, & \text{when } s \le s_c, \\ I_0 e^{-\alpha(s-s_c)}, & \text{when } s > s_c, \end{cases} \end{aligned} \tag{15}$$

where s denotes the charging time, and s_c represents the moment when the charging current transfers from a constant state to an exponential attenuation function. Following the theory for a storage battery, s_c can be determined with the condition that at $s = s_c$, in general, the stored charge in the battery reaches 80 percent of the maximum capacity Q_m. V_0 and V_∞ stand for the initial and the final voltages of the battery, respectively, α is a constant, and I_0 stands for the charging current at the initial charging stage. From the energy conservation theory, (14) and (15), we have

$$I_0 = \begin{cases} \left(V_{\text{rect}}/V_c\right)\langle I_{\text{rect}}\rangle/K, & \text{for } I_0 \le I_m, \\ I_m, & \text{otherwise}, \end{cases} \tag{16}$$

where I_m is the maximal allowable charging current of the rechargeable battery, and $K = 1 + 5(V_c - V_0)/[Q_m(e^4 - 1)]$.

In general, V_{rect} should be fixed at an optimal value to make the inner piezoelectric transducer output maximal power. The battery voltage will be increased gradually with charging the battery, especially for the charging time before 80 percent of the battery maximum capacity is reached. A dc-dc converter is installed to match the optimal rectified voltage V_{rect} with the battery voltage V_b through modulation of its duty cycle.

In the next section, we will focus on analyzing the effect of the energy transmitting process on the performance of the wireless energy supply system in detail in this research; the effect of the dc-dc converter has already been carefully studied by Hu *et al.* in [3], [4].

III. Analysis of the Energy Transmitting Element

We assume the analysis of the 2 piezoelectric transducers for open and closed stages consist of particular and general solutions, as follows:

$$\begin{aligned} u_3^o\left(x_3, t\right) &= u_3^{op}\left(x_3, t\right) + u_3^{og}\left(x_3, t\right), \\ u_3^c\left(x_3, t\right) &= u_3^{cp}\left(x_3, t\right) + u_3^{cg}\left(x_3, t\right), \end{aligned} \tag{17}$$

where and following the superscripts or subscripts "o" and "c" refer to open and closed circuit stages, respectively. The solutions of these 2 stages can be obtained one by one as follows:

A. Solutions for an Open Circuit Stage

The energy transmitting element is driven to vibrate by the external voltage source with some remaining static amount of charge, Q_s, on electrodes of the inner transducer, at the instant of entering an open circuit. We construct the solution by superimposing the $Q_s(t_0)$ component of the solution upon the component caused by the harmonic voltage source. We list below these 2 components:

1) *The Q_s Component* $(u_3^{o1}(x_3), V_p^{o1})$: From (2)–(7), we can get the solutions of an open circuit stage:

$$\begin{aligned} &u_3^{o1+}(x_3) = 0, \quad \phi^{o1+}(x_3) = 0, \\ &u_3^{o1-}(x_3) = -\frac{e_{33}Q_s}{c_{33}C_p h_2}x_3, \quad \phi^{o1-}(x_3) = -\frac{Q_s}{C_p h_2}x_3, \end{aligned} \tag{18}$$

where superscripts "+" and "−" represent the quantities of the outside and inner portions, respectively. $C_p = \bar{\varepsilon}_{33}/h_2$ is an effective capacitor of the inner transducer in Fig. 1, and $\bar{\varepsilon}_{33} = \varepsilon_{33}(1 + k_{33}^2)$, $k_{33}^2 = e_{33}^2/(c_{33}\varepsilon_{33})$, $V_p^{o1} = \phi^{o1-}(-h_2) = Q_s/C_p$.

2) *The Component* $(u_3^{o2}(x_3, t), V_p^{o2}(t))$, caused by $\bar{V}_1 \sin \omega_0 t$, is obtained as follows: without static charge at the electrodes, from (2) and (3), we have

$$\begin{aligned} u_3^{o2+}\left(x_3, t\right) &= \left(a_o^+ \sin\xi_0 x_3 + b_o \cos\xi_0 x_3\right)\sin\omega_0 t, \\ u_3^{o2-}\left(x_3, t\right) &= \left(a_o^- \sin\xi_0 x_3 + b_o \cos\xi_0 x_3\right)\sin\omega_0 t, \end{aligned} \tag{19}$$

where $\xi_0 = \omega_0\sqrt{\rho/\bar{c}_{33}}$. The terms $a_o^\pm$ and b_0 are undetermined constants, and can be solved from (5) and (6). Therefore voltage $V_p^{o2}(t)$ can also be written in harmonic form with amplitude V_{oc} as

$$V_p^{o2}(t) = V_{\mathrm{oc}} \sin\omega_0 t,$$
$$V_{\mathrm{oc}} = -\frac{e_{33}}{\varepsilon_{33}}\left(\tan\xi_0 h_2 \sin\xi_0 h_2 + \cos\xi_0 h_2 - 1\right) b_o. \tag{20}$$

The total displacement and output voltage of the transmitting structure at an open circuit stage are obtained by

$$\begin{aligned} u_3^{op\pm}(x_3,t) &= u_3^{o1\pm}(x_3) + u_3^{o2\pm}(x_3,t),\\ V_p^{op}(t) &= V_p^{o1} + V_p^{o2}(t) = Q_s(t_0)/C_p + V_{\mathrm{oc}}\sin\omega_0 t. \end{aligned} \tag{21}$$

3) *General Solutions:* General solutions of an open circuit stage $u_3^{og\pm}(x_3,t)$ should satisfy (2)–(4), so we take the general solution as

$$\begin{aligned} u_3^{og\pm}(x_3,t) &= \sum_{n=1}^{\infty} T_{on}^{\pm}(t) U_{on}^{\pm}(x_3),\\ T_{on}^{\pm}(t) &= C_{on}^{\pm}\sin\omega_{on}t + D_{on}^{\pm}\cos\omega_{on}t,\\ U_{on}^{\pm}(x_3) &= A_{on}^{\pm}\sin\xi_{on}x_3 + \cos\xi_{on}x_3, \end{aligned} \tag{22}$$

where $\xi_{on} = \sqrt{\rho\omega_{on}^2/\bar{c}_{33}}$. The equations $C_{on}^{+} = C_{on}^{-} = C_{on}$ and $D_{on}^{+} = D_{on}^{-} = D_{on}$ can be obtained from (6). The n-th natural frequency ω_{on} and coefficients $A_{on}^{\pm}$ can be gotten from homogenous boundary conditions and the charge condition. We can solve the output voltage of this part from (4).

B. Solutions for a Closed Circuit Stage

1) Particular Solutions: Since the output voltage of the inner transducer keeps a constant $V_p(t) = V_{\mathrm{rect}}$ in the closed stage, particular solutions consist of a static part and a dynamic part as

$$\begin{aligned} u_3^{cp\pm}(x_3,t) &= u_3^{cs\pm}(x_3) + u_3^{cd\pm}(x_3,t),\\ u_3^{cp+}(x_3,t) &= \left(a_c^{+}\sin\xi_0 x_3 + b_c\cos\xi_0 x_3\right)\sin\omega_0 t,\\ u_3^{cp-}(x_3,t) &= -\frac{e_{33}V_{\mathrm{rect}}}{c_{33}h_2}x_3\\ &\quad + \left(a_c^{-}\sin\xi_0 x_3 + b_c\cos\xi_0 x_3\right)\sin\omega_0 t,\\ V_p &= V_p^{cs} = V_{\mathrm{rect}}, \end{aligned} \tag{23}$$

where coefficients $a_c^{\pm}$ and b_c can be obtained in a way similar to that for (18) and (19), except that electric conditions are changed to $V_p^{cs} = V_{\mathrm{rect}}$, $Q_p^{cs} \neq 0$ for the static part and $V_p^{cd}(t) = 0$, $Q_p^{cd}(t) \neq 0$ for the dynamic part; the static charge Q_p^{cs} and dynamic charge $\bar{Q}_p^{cd}\sin\omega_o t$ can be obtained from (7).

2) General Solutions: General solutions of a closed circuit stage $(u_3^{cg+}(x_3,t), u_3^{cg-}(x_3,t))$ have the same form as the open circuit stage:

$$\begin{aligned} u_3^{cg\pm}(x_3,t) &= \sum_{n=1}^{\infty} T_{cn}(t) U_{cn}^{\pm}(x_3),\\ T_{cn}(t) &= C_{cn}\sin\omega_{cn}t + D_{cn}\cos\omega_{cn}t,\\ U_{cn}^{\pm}(x_3) &= A_{cn}^{\pm}\sin\xi_{cn}x_3 + \cos\xi_{cn}x_3, \end{aligned} \tag{24}$$

where $\xi_{cn} = \sqrt{\rho\omega_{cn}^2/\bar{c}_{33}}$. The terms ω_{cn} and $A_{cn}^{\pm}$ can be solved in a way similar to that for ω_{on} and $A_{on}^{\pm}$, except that the homogenous condition, $\phi(h_1,t) = 0$, for the closed stage in (5) replaces $Q_p = 0$ for the open stage in (7).

C. Solutions of Coefficients $\mathbf{C_{on}}$, $\mathbf{D_{on}}$ and $\mathbf{C_{cn}}$, $\mathbf{D_{cn}}$

From (11) and (12), coefficients of C_{on}, D_{on} and C_{cn}, D_{cn} can be solved; now the current flowing out of the inner transducer at a closed circuit stage can be written as

$$\begin{aligned} i_p^c(t) &= -\left(\dot{Q}_p^{cp} + \dot{Q}_p^{cg}\right)S\\ &= -\bar{Q}_p^{cd}S\omega_0\cos\omega_0 t\\ &\quad + \sum_{i=1}^{\infty}\bar{Q}_{pn}^{cg}S\omega_{cn}\left[C_{cn}\sin\omega_{cn}t - D_{cn}\cos\omega_{cn}t\right], \end{aligned} \tag{25}$$

where S denotes the electroded surface area of the inner transducer and $\bar{Q}_{pn}^{cg}$ can be gotten by substituting (24) into (7).

IV. Numerical Results

Consider PZT-5H as an example. Its mass density $\rho = 7500$ kg/m^3, and the material parameters are as given below [18]:

$$\begin{aligned} (c_{11}, c_{12}, c_{13}, c_{33}, c_{44}) &= (12.6, 7.95, 8.41, 11.7, 2.30)\\ &\quad \times 10^{10}\ \mathrm{N/m^2},\\ (e_{15}, e_{31}, e_{33}) &= (17.0, -6.5, 23.3)\ \mathrm{C/m^2},\\ (\varepsilon_{11}, \varepsilon_{33}) &= (1700, 1470)\varepsilon_0,\\ \varepsilon_0 &= 8.854\times 10^{-12}\ \text{farads/m}. \end{aligned} \tag{26}$$

The frequency of the sinusoidal voltage source is set at $f_0 = 1$ MHz, and the input voltage amplitude $\bar{V}_1 = 10$ V. In our calculations, $h_1 = 1$ mm, $h_2 = 2$ mm, and $S = 0.01$ m^2 are fixed. For the rechargeable battery, $Q_m = 100$ mAh, $I_m = 10$ mA, $V_0 = 1.8$ V, and $V_\infty = 2.31$ V.

The vibration period of the transducer system is $T_0 = 2\pi/\omega_0$. We take $t = T_0/4$ as the beginning point of calculation on an energy transmitting process, because it is known that the deformation of the piezoelectric element arrives at its first positive extremum at $t = T_0/4$ in

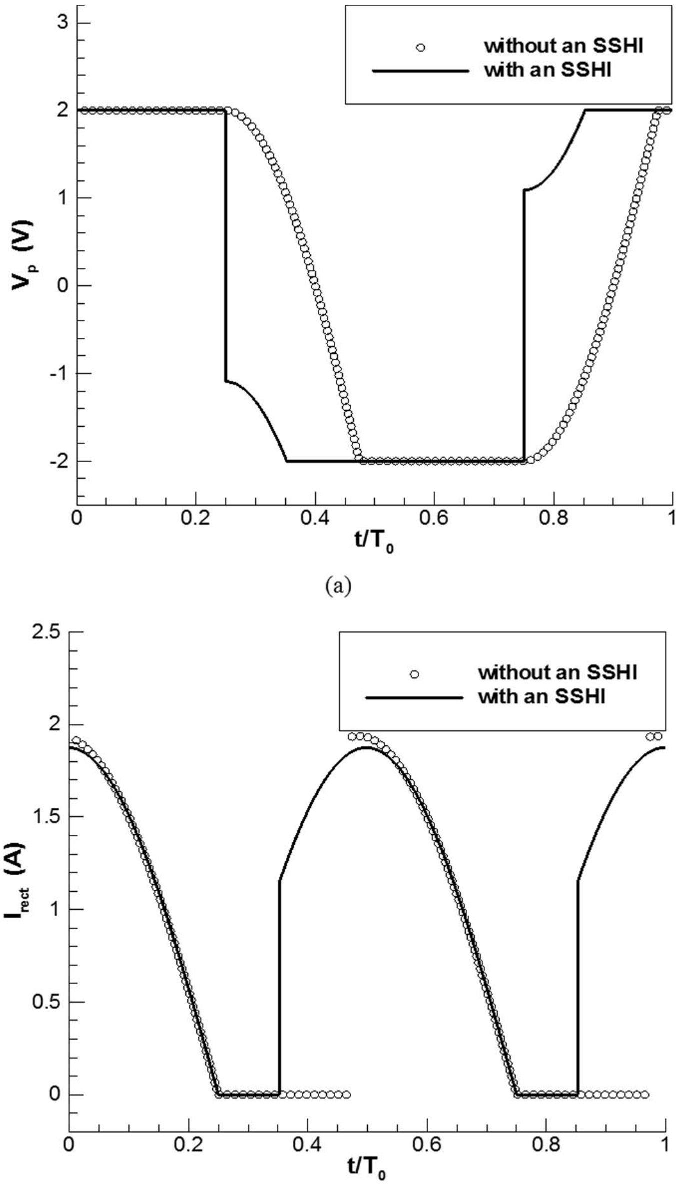

(b)

Fig. 3. (a) Comparison of output voltage, V_p, of the inner transducer versus time over one period T_0 between the energy transmitting element with and without an SSHI. (b) Comparison of output current, i_{rect}, of the rectifier versus time over one period T_0 between the transmitting element with and without an SSHI.

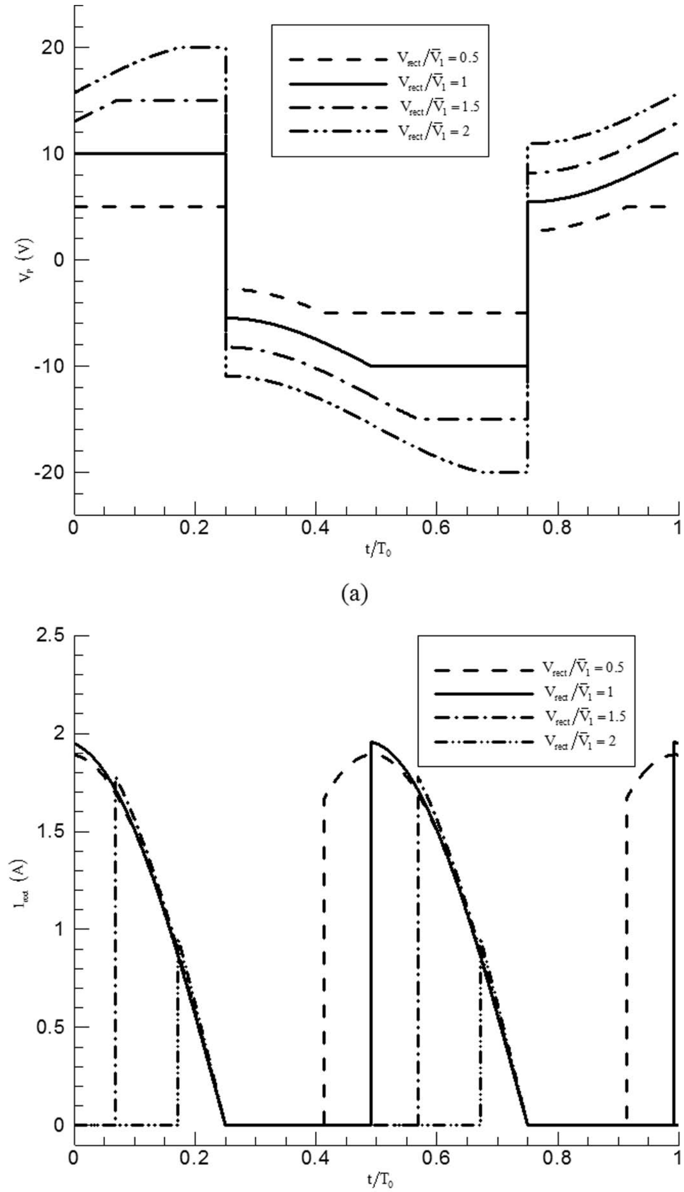

(b)

Fig. 4. (a) Output voltage, V_p, of the inner transducer versus time over one period T_0. (b) Output current, i_{rect}, of the rectifier versus time over one period T_0.

one period T_0; that is, $t = T_0/4$ is a transition point of the rectifier from closed to open circuit [3], [4], [13], [14]. Fig. 3 shows the comparison on the output voltage, V_p, of the inner transducer and the output current, i_{rect}, of the rectifier versus time over one period T_0 with and without an SSHI, where V_{rect} is fixed at 2 V. It should be noted that we have shifted the dependence of V_p and i_{rect} upon t inside $(2\pi/\omega_0, 5\pi/2\omega_0)$ to $(0, \pi/2\omega_0)$ because of the periodicity. It can be seen in Fig. 3 that employing an SSHI in the energy transmitting element largely shortens the open circuit interval and extends the closed circuit interval of the rectifier. Thus, we will focus on studying the energy transmitting element system with SSHI in the following.

Fig. 4 plots V_p and i_{rect} versus the time over one period T_0. We note that a larger V_{rect} results in a shorter closed circuit stage of the rectifier and, conversely, a smaller V_{rect} corresponds to a longer rectifier closed circuit.

Fig. 5 represents the output power of the energy transmitting element versus V_{rect}. There exists an optimal output voltage V_{rect} at which the maximal output energy can be transferred by the energy transmitting element. Considering that this optimal voltage may not be identical to the battery voltage in general, we employ a dc-dc converter following C_{rect} that can match V_{rect} with the battery voltage effectively. Dependence of charging voltage and current upon time are drawn in Fig. 6. It follows from Fig. 6 that there is a time point s_c that divides the

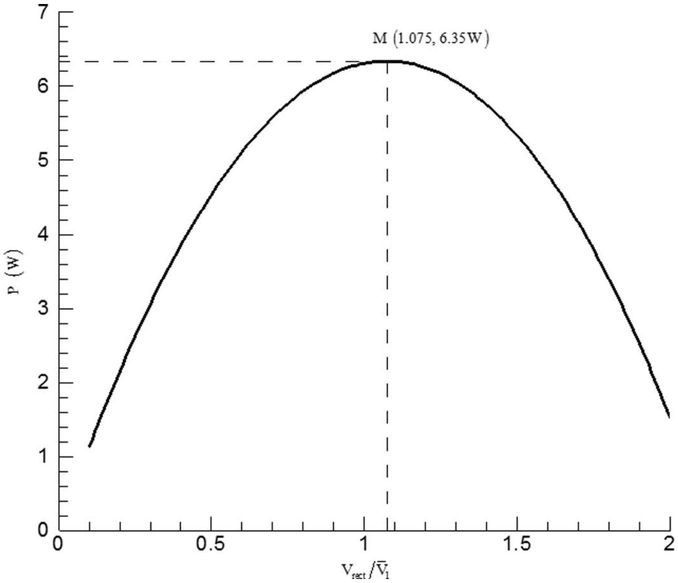

Fig. 5. Output power of the energy transmitting element versus the voltage ratio $V_{\mathrm{rect}}/\bar{V}_1$.

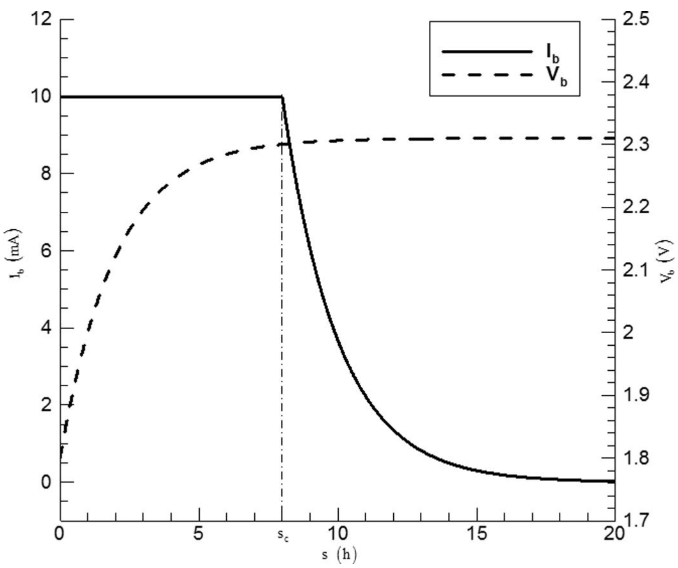

Fig. 6. The current i_b and the voltage V_b of the battery versus time in the whole charging process.

process of charging the battery into 2 stages. A more detailed discussion on energy storage can be found in [4].

V. Conclusion

Electric energy is wirelessly transmitted through a sealed thin metal wall with the thickness-stretch vibration mode of an energy transmitting system consisting of 2 piezoelectric transducers in parallel with an SSHI, and is stored into a rechargeable battery; both are integrated as a whole through a modulating circuit. The process of transmitting energy is computed in detail. Numerical results show that the SSHI can artificially extend the closed circuit interval of the rectifier, and there exists an optimal rectified voltage to make the battery recharge more efficiently.

Acknowledgment

We thank Zengtao Yang in the Department of Engineering Mechanics, University of Nebraska, for helpful discussion.

References

[1] X. Bao, B. J. Doty, S. Sherrit, M. Badescu, Y. Bar-Cohen, J. Aldrich, and Z. Chang, "Wireless piezoelectric acoustic-electric power feedthru," in *Proc. SPIE: Sensors and Smart Structures Technologies for Civil, Mechanical, and Aerospace Systems*, vol. 6529, 2007, artno. 652940.

[2] Y. T. Hu, H. P. Hu, and J. S. Yang, "A low frequency piezoelectric power harvester using a spiral-shaped bimorph," *Sci. China, G*, vol. 49, no. 6, pp. 649–659, 2006.

[3] H. P. Hu, H. Xue, and Y. T. Hu, "A spiral-shaped harvester with an improved harvesting element and an adaptive storage circuit," *IEEE Trans. Ultrason, Ferroelectr. Freq. Contr.*, vol. 54, no. 6, pp. 1177–1187, 2007.

[4] Y. T. Hu, H. Xue, T. Hu, and H. P. Hu, "An energy harvester with an improved piezoelectric harvesting structure and an adaptive storage circuit," *IEEE Trans. Ultrason. Ferroelectr. Freq. Contr.*, vol. 55, no. 1, pp. 148–160, 2008.

[5] Y. T. Hu, X. S. Zhang, J. S. Yang, and Q. Jiang, "Transmitting electric energy through a metal wall by acoustic waves using piezoelectric transducers," *IEEE Trans. Ultrason. Ferroelectr. Freq. Contr.*, vol. 50, no. 7, pp. 773–781, 2003.

[6] Y. T. Hu, C. Y. Chen, X. H. Yang, and Q. G. Du, "Electric energy transmission between two piezoelectric transducers," *Acta Mech. Solida Sinica*, vol. 24, no. 3, pp. 304–312, 2003.

[7] Z. T. Yang, S. H. Guo, and J. S. Yang, "Transmitting electric energy through a closed elastic wall by acoustic waves and piezoelectric transducers," *IEEE Trans. Ultrason. Ferroelectr. Freq. Contr.*, vol. 55, no. 6, pp. 1380–1386, 2008.

[8] S. Sherrit, M. Badescu, X. Bao, and Y. B. Cohen, "Efficient electromechanical network model for wireless acoustic-electric feedthroughs," in *Proc. SPIE Int. Soc. Opt. Eng.*, 2005, pp. 362–372.

[9] S. Sherrit, B. Doty, M. Badescu, and X. Bao, "Studies of acoustic-electric feed-throughs for power transmission through structures," in *Proc. SPIE Int. Soc. Opt. Eng.*, 2006, art. no. 617102.

[10] Z. Chang, X. Bao, B. J. Doty, S. Sherrit, Y. Bar-Cohen, M. Badescu, and J. Aldrich, "Power loss consideration in wireless piezoelectric acoustic-electric power feedthru," in *Proc. SPIE: Sensors and Smart Structures Technologies for Civil, Mechanical, and Aerospace Systems*, 2007, art. no. 652942.

[11] G. J. Saulnier, H. A. Scarton, A. J. Gavens, and D. A. Shoudy, "Through-wall communication of low-rate digital data using ultrasound," in *Proc. IEEE Ultrason. Symp.*, 2006, pp.1385–1389.

[12] R. Primerano, K. Wanuga, J. Dorn, M. Kam, and K. Dandekar, "Echo-cancellation for ultrasonic data transmission through a metal channel," in *Proc. CISS'07: 41st Ann. Conf. on Information Sciences and Systems*, 2007, pp. 841–845.

[13] D. Guyomar, A. Badel, E. Lefeuvre, and C. Richard, "Toward energy harvesting using active materials and conversion improvement by nonlinear processing," *IEEE Trans. Ultrason. Ferroelectr. Freq. Contr.*, vol. 52, no. 4, pp. 584–595, 2005.

[14] Y. C. Shu, I. C. Lien, and W. J. Wu, "An improved analysis of the SSHI interface in piezoelectric energy harvesting," *Smart Mater. Struct.*, vol. 16, no. 6, pp. 2253–2264, 2007.

[15] Y. T. Hu, H. Xue, J. S. Yang, and Q. Jiang, "Nonlinear behavior of a piezoelectric power harvester near resonance," *IEEE Trans. Ultrason. Ferroelectr. Freq. Contr.*, vol. 53, no. 7, pp. 1387–1391, 2006.

[16] H. F. Tiersten, *Linear Piezoelectric Plate Vibrations*, New York: Plenum, 1969.

[17] J. S. Yang, *The Mechanics of Piezoelectric Structures.* Singapore: World Scientific, 2006.

[18] B. A. Auld, *Acoustic Fields and Waves in Solids*, vol. 1. New York: Wiley, 1973, pp. 357–382.

Hongping Hu received his B.S. degree in mechanical engineering from Nanchang University, Nanchang, China, in 1996, and his M.S. degree in environmental engineering in 2003 and his Ph.D. degree in mechanics in 2006 from Huazhong University of Science and Technology, Wuhan, China. His research focuses on the piezoelectric structures and devices, and bubble dynamics.

Yuantai Hu received his B.S. degree in mining engineering in 1986 from Wuhan University of Science and Technology, Wuhan, China, and his M.S. and Ph.D. degrees in mechanics, respectively, from Harbin University of Technology, Harbin, China, in 1988, and from Shanghai Institute of Applied Mathematics and Mechanics, Shanghai University, Shanghai, China, in 1992.

His research area is piezoelectric structures and devices, ultrasonics, and acoustics.

Chuanyao Chen received his B.S. degree in design of aircraft in 1968 from Nanjing Institute of Aeronautics, Nanjing, China.

His research area is solid mechanics.

Ji Wang received his B.S. degree in structural engineering in 1983 from Gansu University of Technology, Lanzhou, Gansu, China. From 1983 to 1988, he was a structural engineer at the 11th Institute of Project Planning and Research in Xi'an, Shaanxi, China. From 1988 to 1990, he was a visiting scientist at Argonne National Laboratory, Argonne, IL, working on structural analysis. From 1990 to 1995, he was a graduate student at Princeton University, Princeton, NJ, studying high frequency vibrations of piezoelectric plates. He received his M.S. and Ph.D. degrees in civil engineering from Princeton in 1993 and 1996, respectively. He was employed by Epson Palo Alto Laboratory, Palo Alto, CA, from 1995 to 1999; NetFront Communications, Sunnyvale, CA, from 1999 to 2001; and SaRonix, San Jose, CA, from 2001 to 2002. Since 2002, he has been a *Qian* River Fellow Professor at Ningbo University, Ningbo, China. His research has been on physical acoustic waves in bulk and surface acoustic wave resonators.